Chapter

Ferroelectric, Piezoelectric and Dielectric Properties of Novel Polymer Nanocomposites

Maheswar Panda

Abstract

In this chapter, the Ferroelectric, Piezoelectric and Dielectric behavior of novel polymer/ceramic nano-composite (PCC) based on ferroelectric polymer [polyvinylidene fluoride (PVDF)] & nano Barium Titanate (n-BaTiO3) with different volume fractions of n-BaTiO3 (f_{BaTiO3}), prepared through the novel cold pressing method has been discussed. The ferroelectric parameters of PCC are attributed to spherulites of PVDF, the increase of n-BaTiO3 and the ordered homogenous structure due to the novel cold pressing. The clustering of ceramic fillers is responsible for randomization of the structures of these composite ferroelectrics for some samples, leading to decrease of electrical polarisations. The piezoelectricity and piezoelectric coefficients of these composites ferroelectrics, increases with increase of ceramic filer content and remains constant beyond a certain ratio. However, the dielectric properties increase linearly as a function of ceramic content due to increase of interfaces/interfacial polarisations. The enhancement of effective dielectric constant (ε_{eff}) is attributed to the large interfacial polarization arising due to the charge storage at the spherulites of PVDF and at the polymer/filler interfaces of PCC and have been explained on the basis of sum effect with the help of the standard models. The achieved lower loss tangent (Tan δ) for the PCC as compared to the polymer/metal composites (PMC) is attributed to the highly insulating nature of PVDF & semiconducting n-BaTiO3. The thermal stability of the composites is also maintained due to the higher melting temperature (170°C) of PVDF. The cold pressed PCC based on PVDF are going to act as better polymer ferroelectric/dielectrics for memory and electrical energy storage applications.

Keywords: Polymer ferroelectrics/dielectrics, spherulites, Ferroelectric polymers, Barium titanate, Dielectric constant, Loss Tangent, Polymer nanocomposites

1. Introduction

Polymer ferroelectrics (PF) and polymer dielectrics (PD) are considered recently to be the fascinating materials for their large inherent benefits of non-volatile memory/sensor/piezoelectric/dielectric/pyroelectric/magneto-electric applications [1–17]. The conventional ferroelectric ceramic materials, e.g. BaTiO3, PZT, PbTiO3, etc. being used as memory elements/piezoelectric sensors/actuators/transducers, etc. are suffering from a large number of disadvantages, such as; brittleness, high cost and consume higher energy/longer time for their preparation.

To overcome these problems, PF are undergoing development based on ferroelectric polymer as well as ferroelectric ceramics. Among the ceramic fillers, BaTiO3 is a very good ferroelectric material and comparably better as others have harmful lead content [16, 17]. Among the various polymers, very few polymers, such as polyvinylidene fluoride (PVDF), polyvinylidene fluoride trifluoroethylene [PVDF Tr(FE)] and Teflon show ferroelectric/piezoelectric behavior and have high dielectric constants [18, 19]. They are also of high breakdown strength, lightweight, flexible and having permanent dipolar polarization. Among the ferroelectric polymers, PVDF shows high piezo-electric coefficients, good ferroelectric behavior. Due to these advantages, PVDF is used as piezo-electric sensors/actuators/memory devices. But the major problem with PVDF is that, the magnitudes of ferroelectric parameters aren't as good as the parameters, obtained from the conventional ceramics, which limit them from direct applications. Similarly the PD are having higher flexibility, non-toxicity, bio-compatibility, low cost, higher visco-elastic properties, etc. [20–31]. Due to their higher energy density/lower loss tangent (Tan δ) with higher breakdown field strength, they are going to be the emerging materials of future for electrostatic energy storage applications. The PD composed of polymers with conductor/ceramic nanoparticles are considered recently to be the demanded materials for electrical energy storage applications [20–36]. For energy storage applications, the maximum stored energy per unit volume is $U = \frac{1}{2} K \varepsilon_0 E_{\max}^2$, where K is the relative dielectric constant and $E_{\max}$ is the maximum electric field, which can be applied to the material (proportional to the breakdown field of the material). Over the last 20 years of research, the ferroelectric polymers e.g PVDF matrix also have been preferred due to it's high static dielectric constant (~15)/higher visco-elastic properties/higher insulating nature as compared to other non-polar polymers. The preferred fillers are high dielectric constant ferroelectric ceramics in development of these PD. However, the development of the polymer-ceramic composites (PCC) have been slowed down, as the effective dielectric constant ($\varepsilon_{\mathrm{eff}}$) for these composites were found be very low i.e. $\varepsilon_{\mathrm{eff}} \sim 100$ at low frequencies due to the low dielectric constant of the polymers as well as due to the conventional hot molding process conditions. In preparing these PCC, ferroelectric ceramic, such as, PMN-PT, BaTiO3, PbTiO3, etc. with varying particle size are introduced into the PVDF matrix through hot molding and partially the approach becomes effective in order to get better PD [5–10]. For preparing PCC based on PVDF, the traditional mixed technique (solution casting followed by hot molding) is used, during which the spherulites of PVDF get lost [2, 33, 34], which lowers the value of $\varepsilon_{\mathrm{eff}}$. Recently Panda et al. [23–30, 32, 33] has shown the importance of spherulites by following the cold pressing technique in preparing the PD based on PVDF, due to which the spherulites of PVDF are retained. The spherulites are responsible in the additional storage of electrical charge due to their additional interfaces, resulting higher interfacial polarization/ higher value of $\varepsilon_{\mathrm{eff}}$ [2, 33, 34].

   With the objective of achieving flexibility with low cost/easy processing and higher value of electrical parameters, for device applications, the traditional process condition (hot molding of the thick films prepared from solution casting) is changed to cold pressing developed by our group in which the spherulites of PVDF will be retained for the case of PCC. Hence, PCC of good ferroelectric/ piezoelectric/dielectric properties, are developed from good ferroelectric ceramics/good ferroelectric polymers. Since in the PZT/PVDF composites, lead is a toxic component, hence the PCC based on PVDF/n-BaTiO$_3$, with different volume fraction of n-BaTiO$_3$ ($f_{n\text{-BaTiO3}}$), were prepared with the help of cold pressing method. The prepared composites have shown the interesting ferroelectric/piezoelectric/ dielectric/conductivity properties and finds suitability for various applications.

2. Experimental details

Polymer composite based on PVDF/n-BaTiO3 from 0.0 to 0.60 of volume fraction of nano filler n-BaTiO3 (f_{BaTiO3}) were prepared by mechanical hand mixing with Agate mortar/Pestle for 2 hours. The final pellets under room temperature consolidation at a pressure of 30 MPa with the help of a Hydraulic press [2, 33] were prepared. The microstructure investigation on the samples was carried out with the help of FESEM. The ferroelectric hysteresis, i.e. the polarization versus electric field (P ~ E) measurement, is done with the help of a P ~ E hysteresis loop tracer. The piezoelectric coefficient (d_{33}) for the samples is measured with the help of Piezo-electric measurement instrument. The electrical measurements were made on all the PCC in the frequency range of 50 Hz to 5 MHz and in the temperature range of room temperature to 100°C. The dielectric results of the PCC have been understood by fitting with the help of the software Mathematica.

3. Results and discussion

3.1 Microstructure

The FESEM micrographs of pure PVDF are given in **Figure 1a** and **b**. **Figure 1a** and **b** shows the presence of spherulites (the spherical semi-crystalline regions of the polymer). The micrographs of PVDF/n-BaTiO3 composites with different f_{BaTiO3} = 0.2 and f_{BaTiO3} = 0.60 are shown (**Figure 1c–f**). The ordered homogenous structures are also observable and is attributed to the recent novel method of cold pressing as evident from the sample with f_{BaTiO3} = 0.2 (**Figure 1c** and **d**). The spherulites present in the polymer are of diameter of the order of ~0.1 μm (**Figure 1a** and **b**). The n-BaTiO3 are also of the order of diameter of the spherulites as they are of size 100 nm, i.e. 0.1 μm, During cold pressing, the n-BaTiO3 clusters (**Figure 1c** and **d**) inside the polymer matrix, may have taken the typical shapes. For the sample with f_{BaTiO3} = 0.6 (**Figure 1e** and **f**), shows high level of heterogeneity, as lot of defects and dislocations has emerged in the structure and is responsible for giving a decrease in the ferroelectric & piezoelectric properties of the PF. **Figure 1** reveal slight agglomeration of BaTiO3 nanoparticles in the nanocomposites. The average filler size in the nanocomposites are of ~100 nm. The nano-dispersion of filler in the polymer matrix is well observed. It is also obvious that a variety of interfaces have occurred into the composites, which will be always useful in the storage of electrical charge at the interfaces The large amount of n-BaTiO3 into the PCC will also be responsible for giving better ferroelectric/piezoelectric/dielectric properties [2, 34–36].

3.2 Ferroelectric properties

3.2.1 Ferroelectric hysteresis

The ferroelectric properties of the PF, prepared from PVDF/n- BaTiO3, the polarization versus electric field (P ~ E) of both the pure materials are given (**Figure 2**) at different voltages. **Figure 2a** shows narrow hysteresis loops for pure PVDF due the mixed phases [α, β, γ, δ & ε] as well as the electrical non-poling of the polymer PVDF.

The polarization versus electric field (P-E hysteresis loop) of the PF under different voltages for various f_{BaTiO3} = 0.2 (**Figure 3a**), f_{BaTiO3} = 0.3 (**Figure 3b**) f_{BaTiO3} = 0.4 (**Figure 3c**) and f_{BaTiO3} = 0.5 (**Figure 3d**) are shown. All the samples show symmetrical P-E hysteresis loops. The loop area increases of with increasing
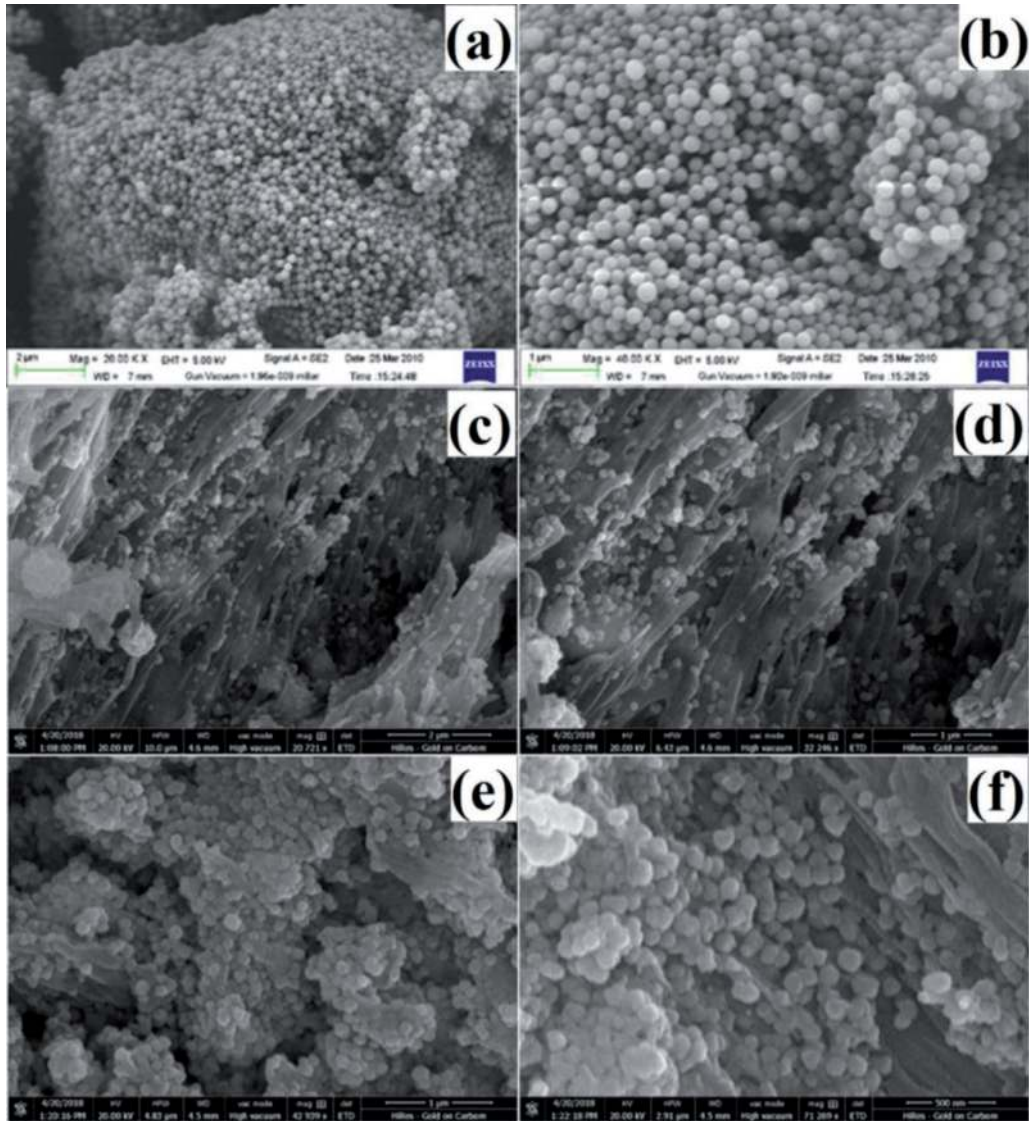
Figure 1.
FESEM micrographs of cold pressed PF (a) pure PVDF (lower resolution) (b) pure PVDF (higher resolution) (c) f_{BaTiO_3} = 0.2 (lower resolution) (d) f_{BaTiO_3} = 0.2 (higher resolution) (e) f_{BaTiO_3} = 0.6 (lower resolution) (f) f_{BaTiO_3} = 0.6 (higher resolution).

the dc voltage from 5 kV to 10 kV. A comparison of P-E hysteresis loops, demonstrate that the samples with f_{BaTiO_3} = 0.2 & 0.3 shows better ferroelectric hysteresis (higher hysteresis loop area) as compared to f_{BaTiO_3} = 0.4 & 0.5. For precise assessment, the hysteresis loops at 8 kV for all the samples shows that the hysteresis loop area increases as a function of f_{BaTiO_3}, up to 0.30 (**Figure 1a–d**). On the other hand, beyond f_{BaTiO_3} = 0.30, the heterogeneity/disordered structure is accountable for the decrement of ferroelectric properties and that is also accredited to the clustering of n-BaTiO3 into the polymer medium (**Figure 1e** and **f**). It is also experiential that with rising the field, the saturation polarization (P_s), remnant polarization (P_r) and the coercive field (E_c) also increases as a function of f_{BaTiO_3} and the finest result is obtained for the sample with f_{BaTiO_3} = 0.3.

To have a thorough analysis and cross examination of the ferroelectric behavior of the PF, the P-E hysteresis loop of all the samples as a function of f_{BaTiO_3} for different fields from 5 kV/cm to 8 kV/cm is shown in **Figure 4**. At all the fields, the ferroelectric behavior from the P-E hysteresis loops, are characterized by the change of P_r, P_s and E_c.
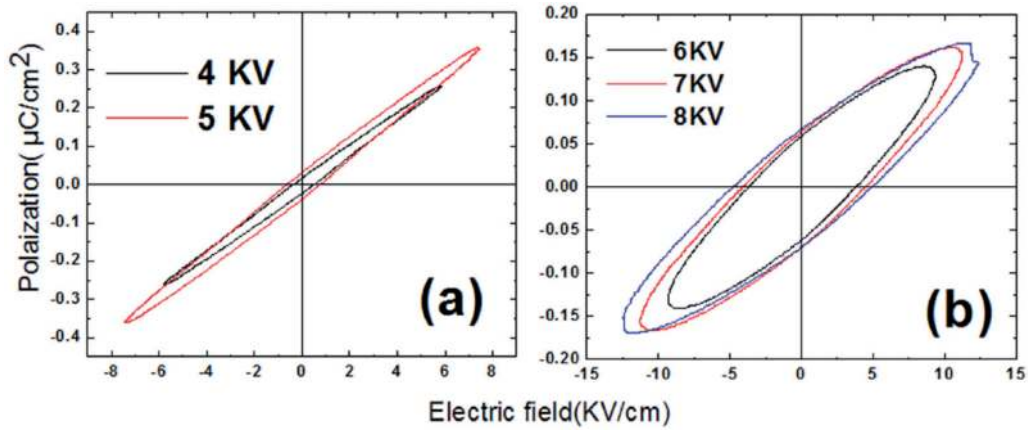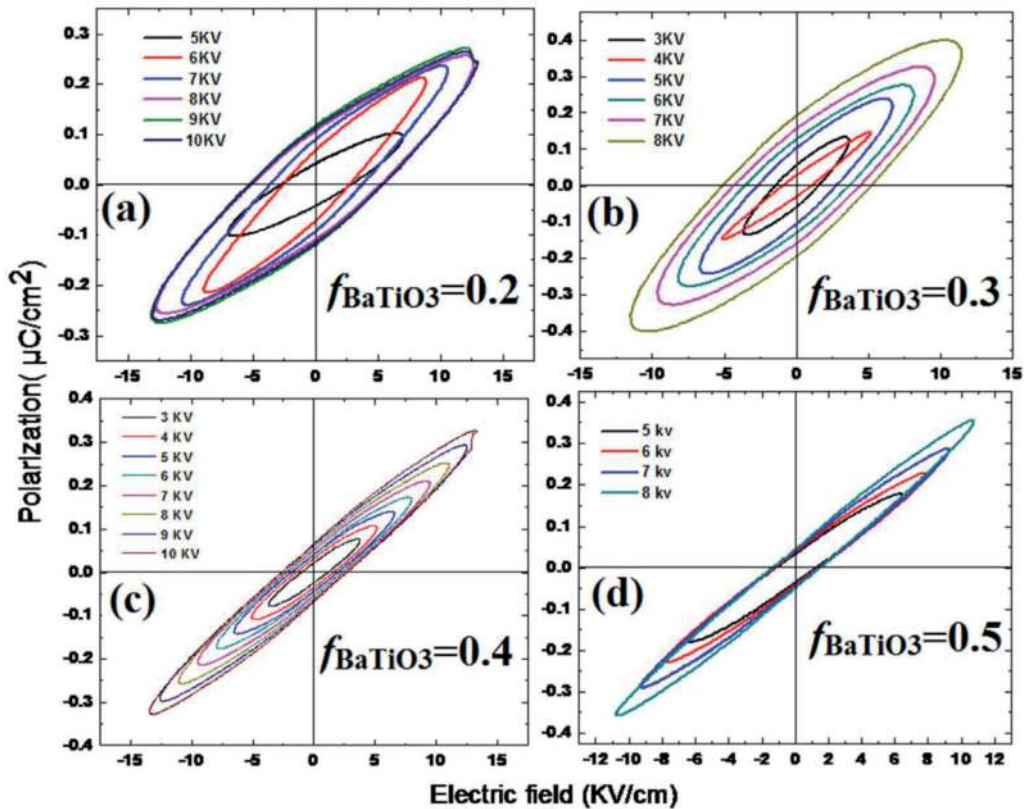
Figure 2.
(color online) polarization (P) vs. applied electric field (E) hysteresis loop measured at a frequency of 1 Hz with different voltages for pure (a) PVDF (b) n-BaTiO3.

Figure 3.
(color online) polarization (P) vs. applied electric field (E) hysteresis loop measured at a frequency of 1 Hz with different fields for different f_{BaTiO_3} (a) 0.20 (b) 0.30 (c) 0.40 (d) 0.50.

The experimental observation is that with increasing of the f_{BaTiO_3} in the PF, the P_r, P_s and E_c also increases. This obviously indicates that the addition of n-BaTiO3 enhances the ferroelectric nature of the polymer material. But when the amount of n-BaTiO3 filler content improved, there is trivial agglomeration of filler in the PVDF matrix. The agglomeration of n-BaTiO3 act as hindrances, which eliminate PVDF Polymer from flowing into the BaTiO3 agglomerates and the aggregated filler causes poor enhancement in ferroelectric nature (decrement in
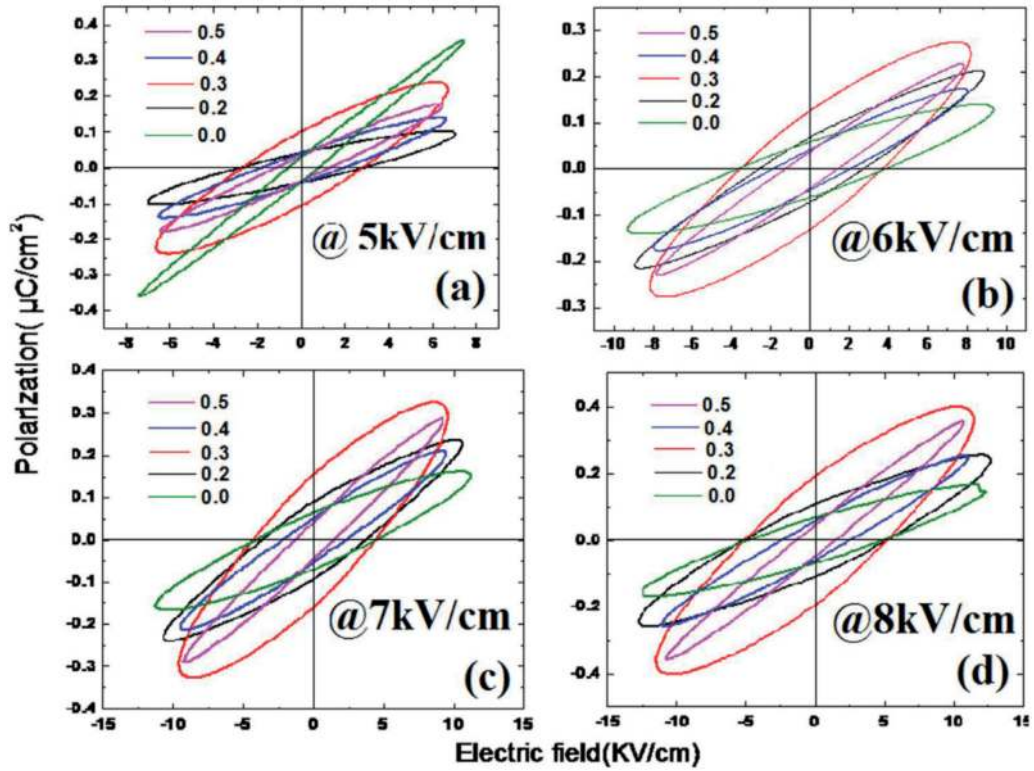
Figure 4.
(color online) polarization (P) vs. applied electric field (E) hysteresis loop measured at a frequency of 1 Hz with different f_{BaTiO3} for different fields (a) 5 kV/cm (b) 6 kV/cm (c) 7 kV/cm (d) 8 kV/cm.

the ferroelectric polarization) as evident from **Figure 4**. Conversely the dielectric properties, such as the effective dielectric constant (ε_{eff}) and loss tangent (Tan δ) of all the PF becomes a linear dependence of f_{BaTiO3} (**Figure 5**), i.e. the static ε_{eff} enhances from 10 for pure PVDF to 400 for f_{BaTiO3} = 0.6, whereas the loss tangent increases from 0.09 for pure PVDF to 0.9 for f_{BaTiO3} = 0.6 [14]. The variation in the dielectric and ferroelectric behavior is credited to the different types of structures responsible for the two altered electrical properties respectively. The dielectric properties are connected with the more interfaces in the PF, hence ε_{eff} & Tan δ enhances linearly with f_{BaTiO3} and the ferroelectric properties are associated with the ordered structure of the PF.

3.2.2 $P_s \sim f_{BaTiO3}$ for different fields

Figure 6 give you an idea about the variation of P_s as a function of f_{BaTiO3} for all the PF, at changed electric fields from 5 kV/cm to 8 kV/cm. It is practical that on increasing the concentration of n-BaTiO3, and also on rising the electric fields, the value of P_s raises up to f_{BaTiO3} = 0.30, but for f_{BaTiO3} > 0.30, P_s decreases, due to the aggregation of n-BaTiO3 causing poor improvement of the ferroelectric properties. At 5 kV/cm, the value of P_s increases from 0.1 µC/cm^2 for f_{BaTiO3} = 0.2 up to 0.24 µC/cm^2 for f_{BaTiO3} = 0.30, but when f_{BaTiO3} > 0.30, P_s decreases to 0.24 µC/cm^2.

3.2.3 $P_r \sim f_{BaTiO3}$ for different fields

The variation of P_r as a function of f_{BaTiO3} for all the PF (**Figure 7**), at different electric fields from 5 kV/cm to 8 kV/cm. It can be seen that on increasing the concentration of n-BaTiO3, P_r increases up to f_{BaTiO3} = 0.30, but for f_{BaTiO3} > 0.30,
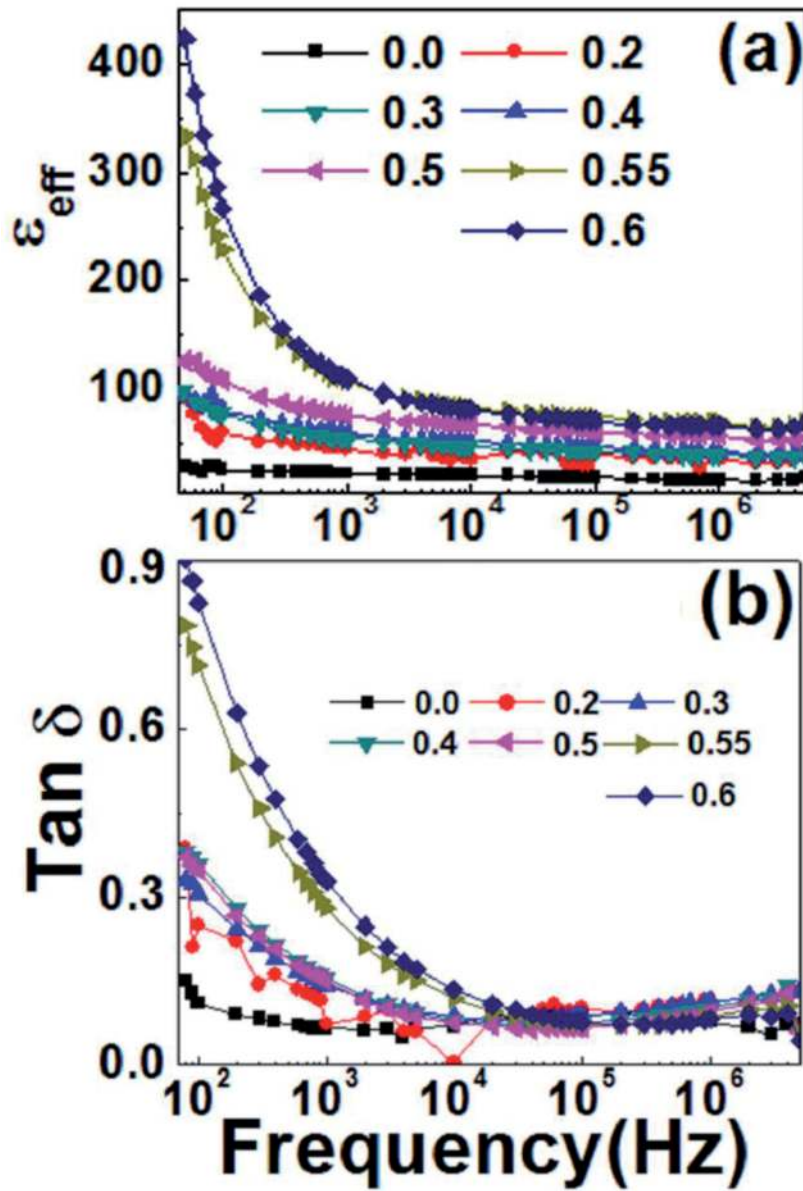
Figure 5.
(color online) the variation of (a) ε_{eff} and (b) tan δ as a function of frequency at 300 K for the PF.

P_r decreases, i.e. a parallel behavior as observed in the case of variation of $P_s \sim f_{BaTiO3}$, is also observed which is attributed to the same origin. At 8 kV/cm, P_r increases from 0.10 µC/cm^2 for f_{BaTiO3} = 0.2 up to 0.20 µC/cm^2 for f_{BaTiO3} = 0.30, but for f_{BaTiO3} > 0.30, P_r decreases and approaches to much less than 0.20 µC/cm^2.

3.2.4 $E_c \sim f_{BaTiO3}$ for different fields

The variation of E_c as a function of f_{BaTiO3} for all the PF, at different electric fields from 5 kV/cm to 8 kV/cm is shown in **Figure 8**. The value of E_c is preserved higher up to f_{BaTiO3} = 0.30, but for f_{BaTiO3} > 0.30, E_c decreases, i.e. a similar conduct as observed in the case of variation of $P_s \sim f_{BaTiO3}$, is also observed endorsed to the same origin. At 6 kV/cm, the value of E_c increases from 2.5 kV/cm for f_{BaTiO3} = 0.2 up to 3.5 kV/cm for f_{BaTiO3} = 0.30, but for f_{BaTiO3} > 0.30, E_c decreases and becomes much less than 3.5 kV/cm.
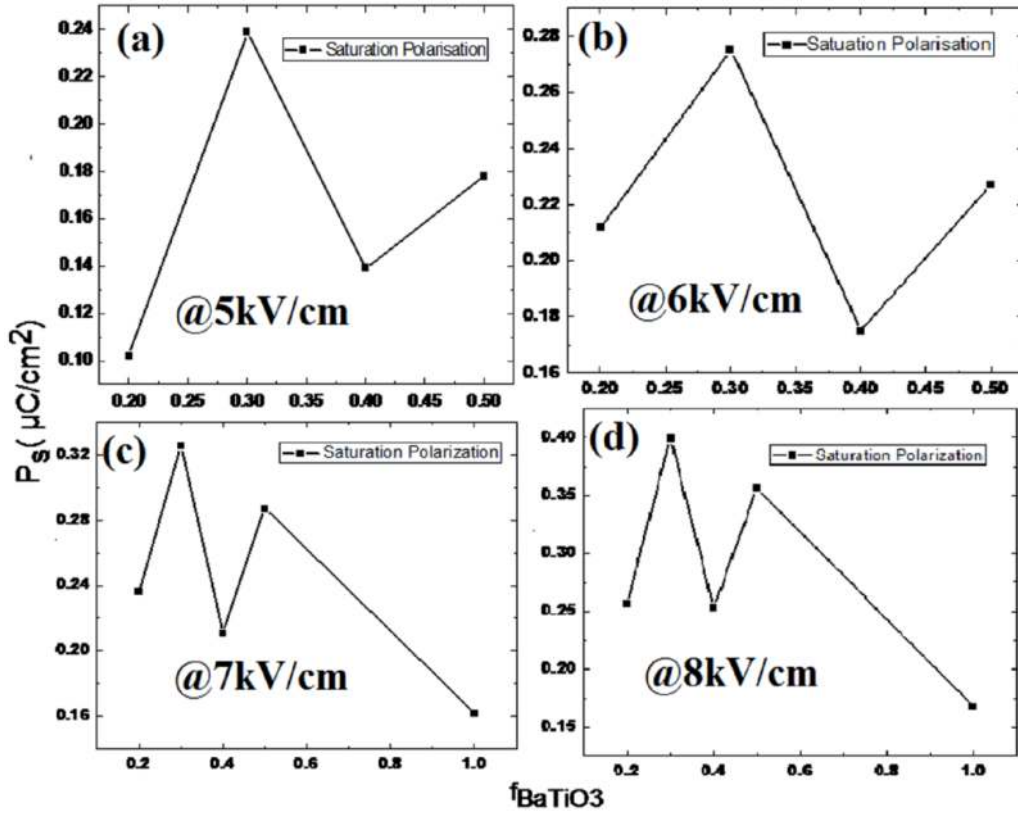
Figure 6.
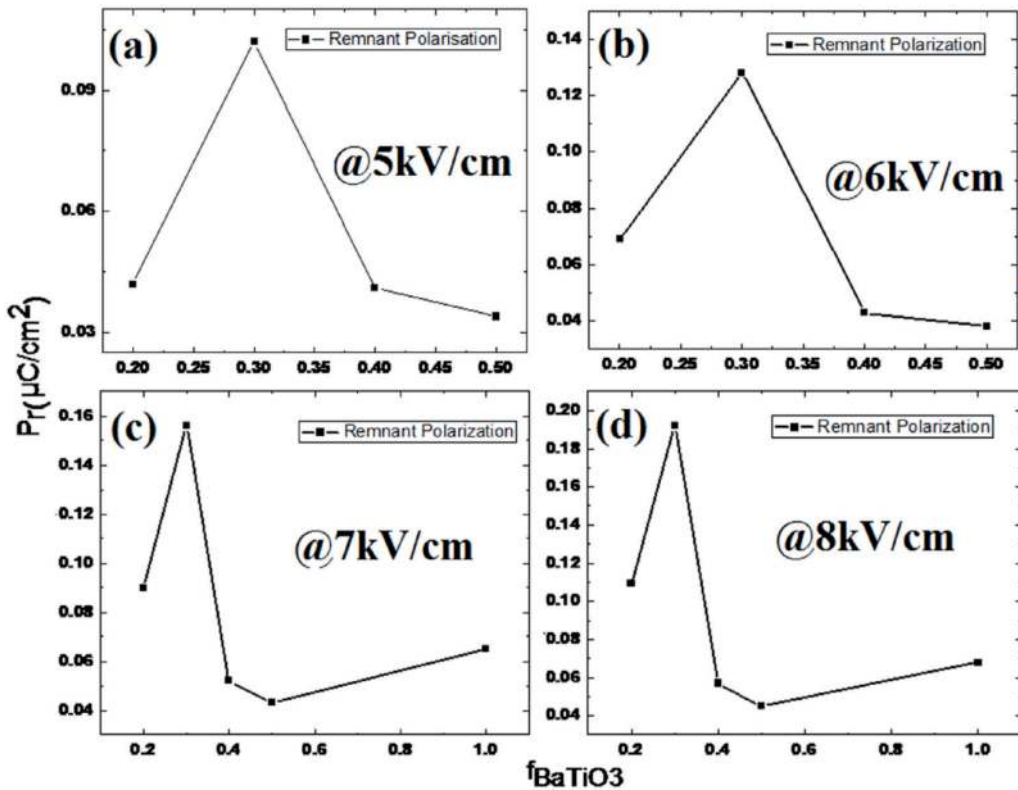$P_s \sim f_{BaTiO_3}$ at different electric fields (a) 5 kV/cm (b) 6 kV/cm (c) 7 kV/cm (d) 8 kV/cm.

Figure 7.
$P_r \sim f_{BaTiO_3}$ at different electric fields (a) 5 kV/cm (b) 6 kV/cm (c) 7 kV/cm (d) 8 kV/cm.
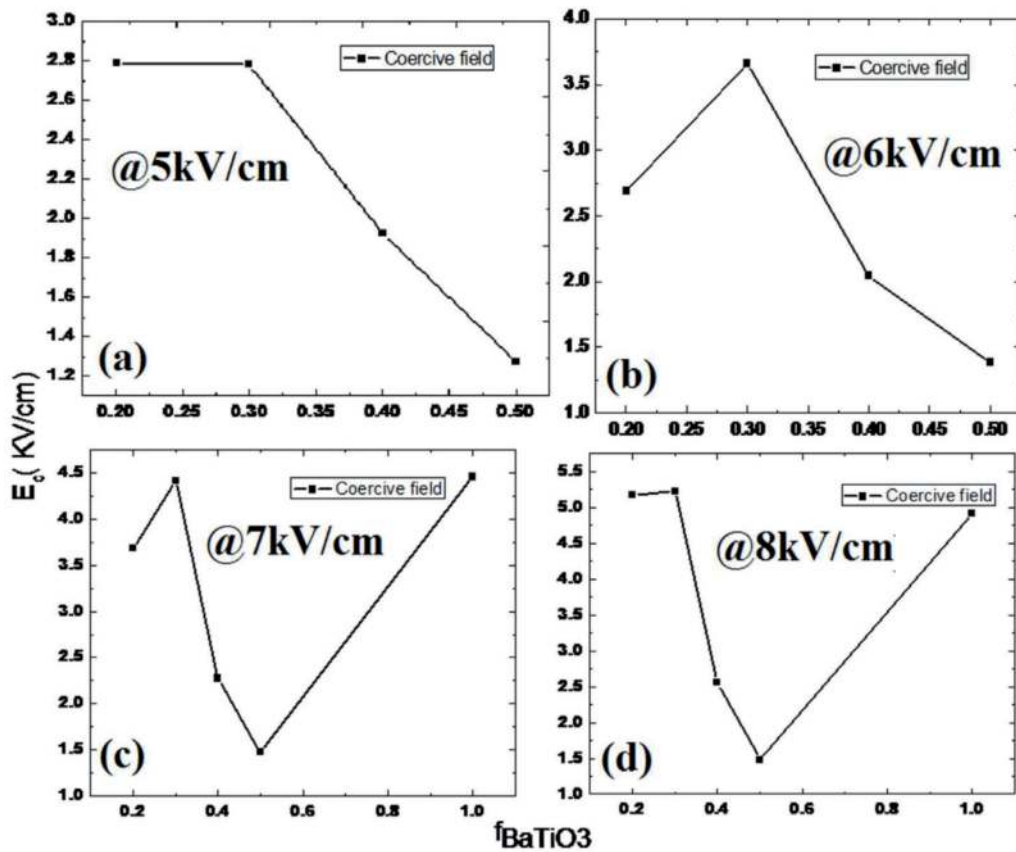
Figure 8.
$E_c \sim f_{BaTiO_3}$ *at different electric fields (a) 5 kV/cm (b) 6 kV/cm (c) 7 kV/cm (d) 8 kV/cm.*

3.3 Piezoelectric properties

Figure 9 gives the explanation of change in piezo- electric coefficient (d_{33}) of the PF as a function of f_{BaTiO3}. On increasing the concentration of n-BaTiO3, the piezoelectric nature of composite also increases and when the amount of n-BaTiO3 filler content increases much, the value of d_{33} becomes constant. The value of d_{33} increases from 2.10 pC/N for f_{BaTiO3} = 0.0 up to 2.20 pC/N for f_{BaTiO3} = 0.20 and remains constant, beyond f_{BaTiO3} = 0.20 up to f_{BaTiO3} = 1.0 because of the aggregated filler (n-BaTiO3) causes poor improvement in the peizo- electric nature of the PF.

3.4 Dielectric properties

The variation of dielectric properties of the PCC as a function of frequency at 300 K are shown in **Figure 10a** and **b**, respectively. The value of ε_{eff} at 50 Hz for the 0.0 sample is 16 while this value increases up to 120 linearly up to the PCC with f_{BaTiO3} = 0.5 & after that it raises up to the value of 330 & 420 for the samples with f_{BaTiO3} = 0.55 & f_{BaTiO3} = 0.60 respectively. The higher value of ε_{eff} for the f_{BaTiO3} = 0.55 & f_{BaTiO3} = 0.60 are attributed to the large interfacial polariza-tion arising due to the occurrence of spherulites and created large interface like structures(during cold pressing), while the spherulites are lost for the hot molded samples (**Figure 11**).

The static dielectric constant (ε_r) of the cold pressed pure PVDF is ~16 i.e. higher than the ε_r of hot molded pure PVDF (~10) due to the loss of spherulites (Inset, **Figure 11**) of the polymer. ε_{eff} decreases with increase of frequency due to the
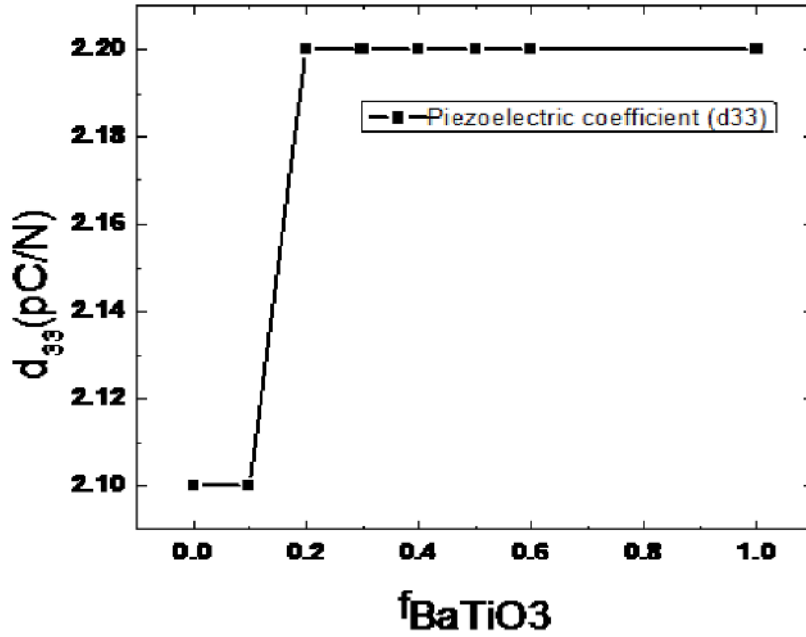
Figure 9.
Variation of the piezoelectric coefficient (d_{33}) as a function of f_{BaTiO3}.

absence of contribution from interfacial polarization at higher frequencies, where only the involvement from dipolar and atomic polarization exists. A very low Tan δ for the PCC with f_{BaTiO3} = 0.6 (having highest ε_{eff} = 420 observed at 50 Hz) was approached to 0.9 at 50 Hz and that also decreases with increase of frequency and the tendency of decrement is also observed for all the PCC. Nevertheless, in the cold pressed PMC [33], the Tan δ was reported to be 10 at 50 Hz (Inset, **Figure 10b**) for the percolative sample, with ε_{eff} ~ 2000. The PMC at f_c shows 10 times higher value of Tan δ in contrast to the result of PCC, although both type of polymer composites are prepared by the same cold pressing procedure. **Figure 12** shows thebehaviour of ε_{eff}, σ_{eff} and Tan δ of the composites as a function of f_{BaTiO3} at different frequencies. The ε_{eff} rises linearly from 16 to 120 for f_{BaTiO3} rises from 0.0 to 0.50 at 100 Hz, due to the large interfacial polarization occurring due to the presence of spherulites. The interfaces formed at the PCC, increases ε_{eff} largely from 120 to 350 & 420 for f_{BaTiO3} = 0.55 & 0.60 respectively. The expression developed by Yamada et al. (which is a model for explaining the sum properties of the composite) was fitted to the dielectric data (**Figure 12(b)**) at 1 kHz frequency. The model is given by

$$\varepsilon_{eff} = K_{PVDF}\left[1 + \frac{nf_{BaTiO3}\left(K_{BaTiO3} - K_{PVDF}\right)}{nK_{PVDF} + \left(K_{BaTiO3} - K_{PVDF}\right)\left(1 + f_{BaTiO3}\right)}\right] \qquad (1)$$

where ε_{eff} is the effective dielectric constant of the composite, K_{PVDF} and K_{BaTiO3} are the dielectric constants of the polymer matrix and the ceramic, respectively, f_{BaTiO3} is the volume fraction of the ceramic and 'n' is a parameter related to the geometry of ceramic particles [2]. K_{PVDF}, K_{BaTiO3} and n found from the fitting of Eq. (1) to the dielectric data are 17, 1600 and 10, is in good agreement with the earlier literature [5].

The σ_{eff} & Tan δ increases with the increase of f_{BaTiO3} in the PCC slowly, suggesting the semiconducting nature of the BaTiO3 nano-ceramics. For f_{BaTiO3} = 0.6, the σ_{eff} value varies within $10^{-8}\ \Omega^{-1}\ cm^{-1}$ to $10^{-4}\ \Omega^{-1}\ cm^{-1}$ for frequency varying between 50 Hz to 5 MHz, while the value of Tan δ is maintained in between 0.1 to 0.9.

Figure 10.
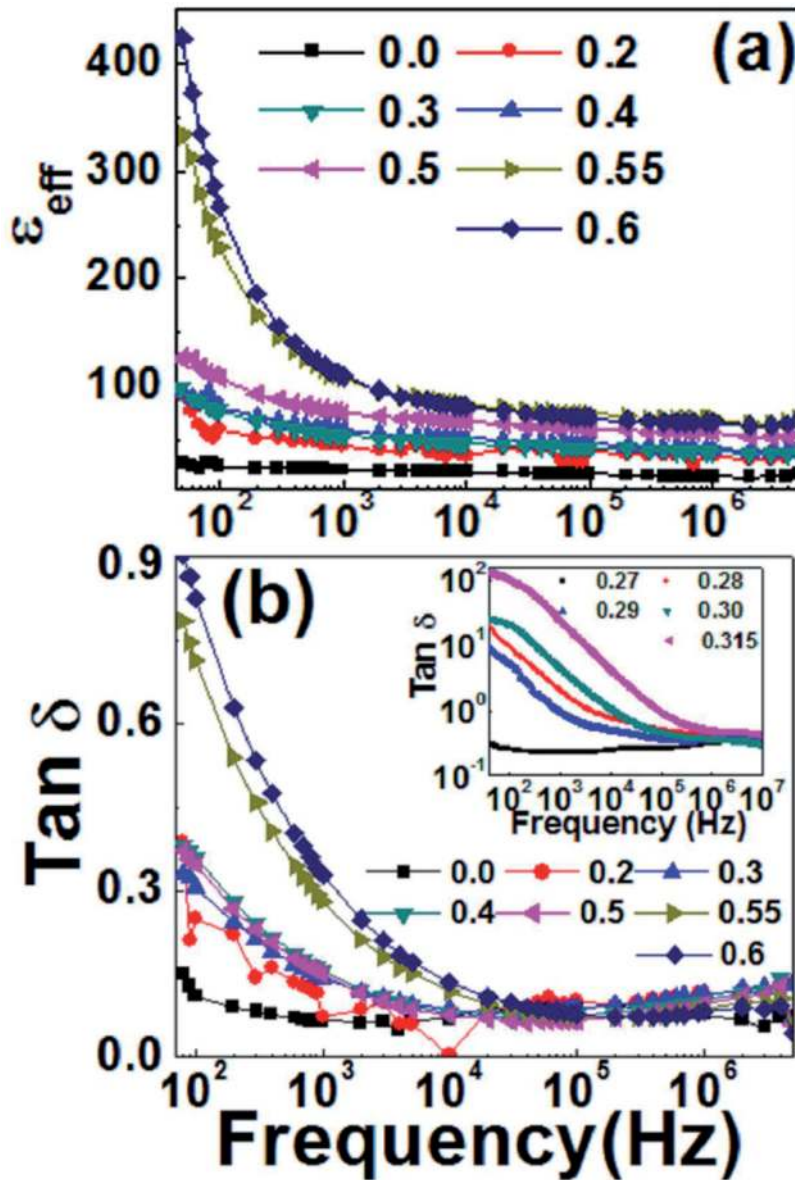*(color online) the variation of (a) ε_{eff} and (b) tan δ as a function of frequency at 300 K for the PD, inset: Tan δ ~ frequency for some typical percolative PMC samples showing higher tan δ [33].*

σ_{eff} & Tan δ are also found to be increasing with increase of frequency, suggesting conventional hopping conduction in the disordered PCC. Similarly, σ_{eff} value was found to be very low i.e. less than $10^{-4}\ \Omega^{-1}$ for all the PCC and that value remains constant over the entire frequency range. The Tan δ raises slowly as a function of f_{BaTiO3} is found to be less than 0.9 even with the PCC having f_{BaTiO3} = 0.6.

The electrical parameters as a function of temperature of the PCC was confirmed by measuring and are given in **Figure 13**. For f_{BaTiO3} = 0.4 (**Figure 13a**) & f_{BaTiO3} = 0.50 (**Figure 13b**), the low frequency (50 Hz) value of ε_{eff} is sustained at a thermal stabilized value of 90 & 130 (with their corresponding decrement as a function of frequency) as a function of temperature from 40–100°C. The stabilization of ε_{eff} is ascribed due to the major effective contribution coming from the sum properties of the dielectric constant of both the components. Yet, for the samples with f_{BaTiO3} = 0.55 &0.6, the reached ε_{eff} ~ 350 & 420 value arises due to the sum properties
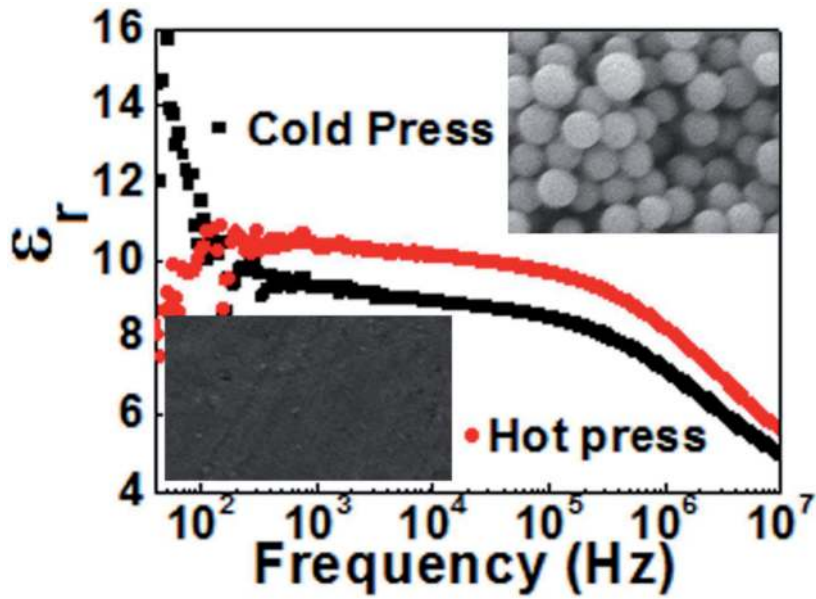
Figure 11.
The variation of dielectric constant (ε_r) with frequency for both cold and hot press PVDF, inset: The FESEM micrograph of the cold/hot molded PVDF showing the presence/loss of spherulites at temperature higher than the room temperature.
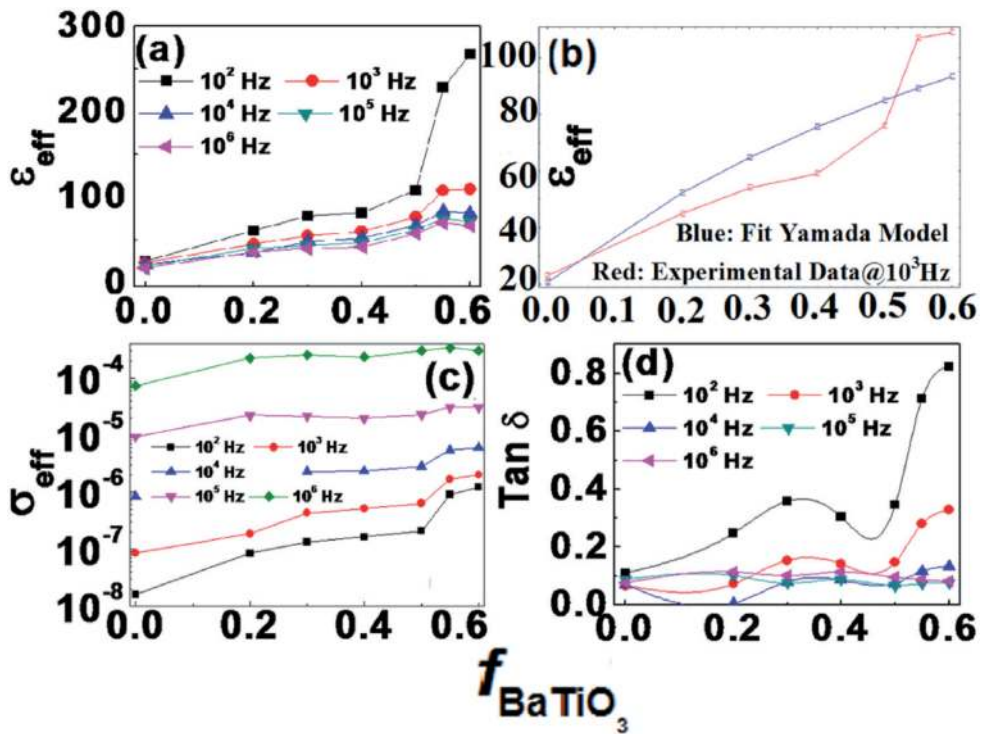

Figure 12.
(color online) the variation of (a) ε_{eff} experimentally (b) fitting of ε_{eff} experimental data at 1KHz with Yamada model as a function of f_{BaTiO_3} (c) σ_{eff} and (d) tan δ as a function of f_{BaTiO_3} for various frequencies at 300 K.

of the dielectric constant of both the components as well as also due to the major contribution of the spherulites. Hence with the rise of temperature, the ε_{eff} decreases due to the deteriorating of the spherulites of the PCC (**Figure 13c** and **d**). Hence the spherulites are useful at room temperature in case of PCC for realizing high value of ε_{eff} with lower Tan δ.
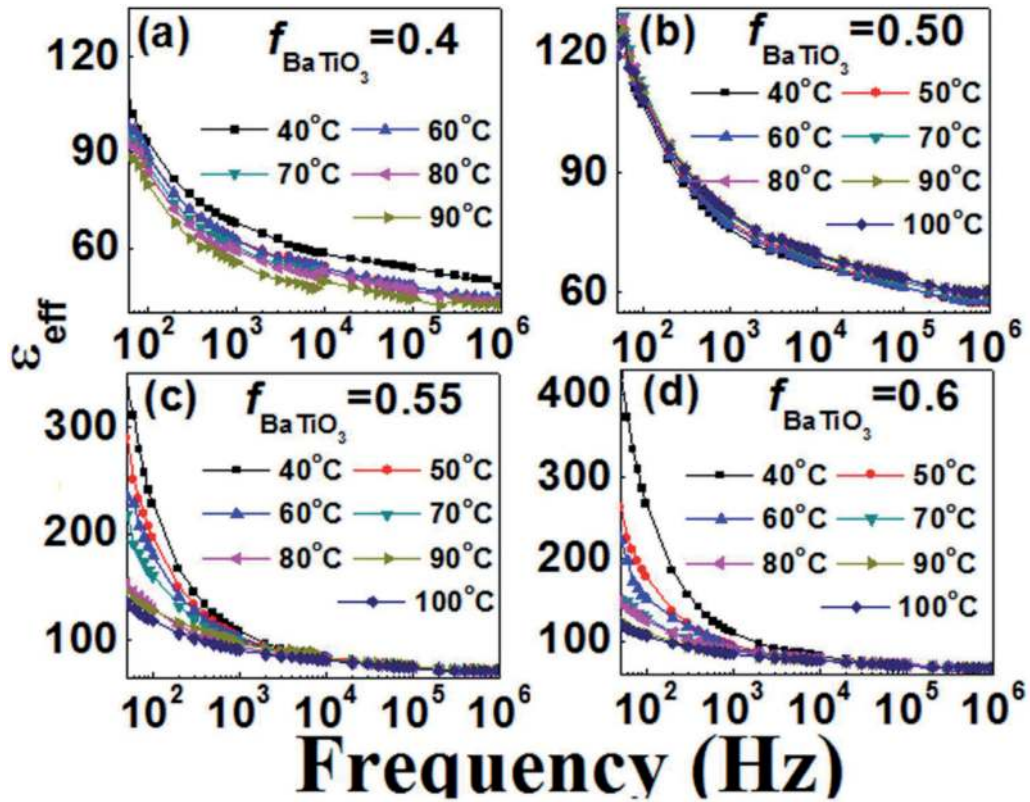
Figure 13.
(color online) the variation of ε_{eff} as a function of frequencies for the temperature varying from 40°C to 100°C for varying f_{BaTiO_3} (a) 0.40 (b) 0.50 (c) 0.55 (d)) 0.60.

3.5 Electrical conductivity

Ac conductivity ($\sigma_{ac} = \omega\varepsilon_0\varepsilon Tan\delta$) as a function of frequency at different f_{BaTiO3} is shown in **Figure 14**. The σ_{eff} as a function of frequency was found to be the ac hoping conduction satisfying the Johnscher's fractional power law. The plot shows dispersion of ac conductivity with frequency corresponding to $f_{BaTiO3} \leq 0.20$, be in agreement with Eq. (2) i.e.

$$\sigma_{ac}(\omega) = \sigma_{dc} + A\omega^k \qquad (2)$$

with the σ_{dc} part becoming zero and the value of $k \sim 1$. The non-presence of dc conductivity for the samples with $f_{BaTiO3} \leq 0.20$, can be understand as the non-presence of percolating paths (being formed from the semiconducting $BaTiO3$ nano-ceramics in the PVDF matrix) due to insufficient fraction of $BaTiO3$. The long rage dc conduction starts to develop for f_{BaTiO3} = 0.3 to 0.5, but a good fit of Eq. (2) could not be resulted for them as the percolating paths were not sufficient. Interestingly, for $f_{BaTiO3} \geq 0.55$, a mixed conductivity is found. The plateau due to the appearance of long range dc conductivity. At higher frequency the conductivity becomes more or less with f_{BaTiO3} dependent. This "hopping or critical frequency ω_H." at which the change in slope takes place can be observed to be increasing with the increase of f_{BaTiO3}, since the length of dc plateau increases with increase of f_{BaTiO3} from 0.3 to 0.6. On the other hand, the value of 'k' lies well within the Johnscher's universal regime [0,1] symptomatic of the validity of Johnscher's power law universally.
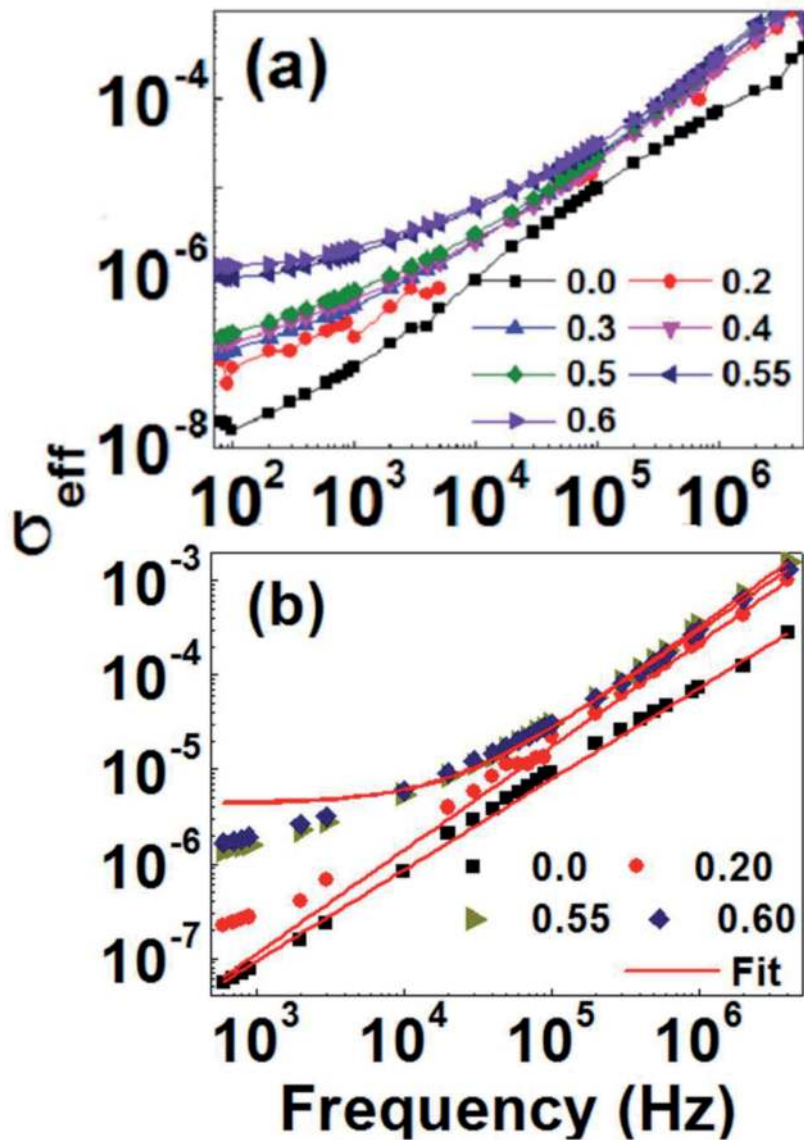
Figure 14.
(color online) the variation of (a) σ_{eff} experimentally and (b) σ_{eff} fitted with Johnscher's power law, as a function of frequencies.

3.6 Conclusions

The micro-structural, ferroelectric, piezoelectric, dielectric and conductivity properties of the polymer composites have been analyzed and are correlated. The properties strongly depend on the novel cold pressing preparation techniques and the dispersion of n-BaTiO3 filler particles into the PVDF matrix and also on the nano-sizes of ceramics. The addition of n-BaTiO3 enhances the ferroelectric, piezoelectric and dielectric properties of the composites. It is also found that this cold pressing method is more suitable to the PCC based on PVDF matrix (since very low value of Tanδ is observed). The spherulites present in PVDF matrix are always helpful in maintaining the dielectric constant and increasing the ε_{eff} of PCC. The enhancement of dielectric results are explained with the help of standard Yamada model. The mixed conductivity appears for the PD/PF and Jonschers universal fractional power law is well satisfied for all composites. The hoping conduction in these disordered materials have been confirmed in all PCC. The dynamics of

charge carriers are filler/temperature dependent. These PD/PF should be explored for applications by focusing the research on achieving lowered Tan δ, which will increase the dielectric field strength/high energy density and better ferroelectric/ piezoelectric properties may be expected for various multifunctional applications.

Author details

Maheswar Panda
Department of Physics, Dr. Harisingh Gour Vishwavidyalaya (A Central University), Sagar, M.P., India

*Address all correspondence to: panda.maheswar@gmail.com

IntechOpen

References

[1] M. E. Lines, and A. M. Glass, Principles and Applications of Ferroelectrics and Related Materials, (Oxford: Clarendon Press, 2001), Vol. 680.

[2] M. Panda and A. Trivedi, Ferroelectric and Piezoelectric Properties of Cold Pressed Polyvinyledene fluoride/Barium Titanate Nano-composites, Ferroelectrics, 572, 246 (2020).

[3] G. A. Kontos, A. L. Soulintzis, P. K. Karahaliou, G. C. Psarras, S. N. Georga, C. A. Krontiras, and M. N. Pisanias, Electrical relaxation dynamics in TiO_2/polymer matrix composites. *Expr. Poly. Lett.* **1**, 781 (2007).

[4] U.Valiyaneerilakkal, and S. Varghese, Poly (vinylidene fluoride-trifluoro-ethylene)/barium titanate nano-composite for ferroelectric nonvolatile memory devices, *AIP Advances* **3**, 042131 (2013).

[5] R. Sharma, I. P. Singh, A. K. Tripathi, and P. K. C. Pillai, Charge-field hysteresis of BaTiO3: PVDF Composites *J. Mat. Sci.* **29**, 995 (1994).

[6] M. Kuhn, and H. Kliem; Monte Carlo Simulations of Ferroelectric Properties for PVDF and BaTiO3; *Ferroelect.* **370**, 207 (2008).

[7] S. Baryshnikova, A. Milinskiya, and E. Stukovab, Dielectric properties of the ferroelectric composites [AgNa (NO2)2]0.9/[NaNO2]0.1 and [AgNa (NO2)2]0.9/[BaTiO3]0.1, *Ferroelectr.* **536**, 91 (2018).

[8] X.F.Li, H.S.Zha, P.L.Zhang, and W.L.Zhong, Composite Films OF BaTiO, and PVDF, *Ferroelectr.* **196**, 39 (1997).

[9] K. Prasad,A. Prasad,K. P. Chandra, and A. R. Kulkarni, Electrical Conduction in 0-3 BaTiO3/PVDF Composites, *Integr Ferroelectr.* **117**, 55 (2010).

[10] D. Olmos, G. Gonzalez-Gaitano, A. L. Kholkin, and J. Gonzalez-Benito, Flexible PVDF-BaTiO3 Nanocomposites as Potential Materials for Pressure Sensors; *Ferroelect.* **447**, 9 (2013).

[11] B. Hilczer, J. Kulek, M. Polomska, M. D. Glinchuk,2 A. V. Ragulya, and A. Pietraszk, Dielectric and Pyroelectric Response of BaTiO3-PVDF Nano-composites; *Ferroelect.* **316**, 31 (2005).

[12] H.-I. Hsiang, K.-Y. Lin, F.-S. Yen, and C.-Y. Hwang, Effects of particle size of BaTiO3 powder on the dielectric properties of BaTiO3/polyvinylidene fluoride composites, *J. Mater. Sci.* **36**, 3809 (2001).

[13] R. Gregorio, Jr., M. Cestari, and F. E. Bernardino, Dielectric behaviour of thin films of β-PVDF/PZT and β-PVDF/BaTiO₃ composites, *J. Mater. Sci.* **31**, 2925 (1996).

[14] H. Kim, F. Torres, D. Villagran, C. Stewart, Y.G. Lin, T. Liang, and B. Tseng, 3D Printing of BaTiO3/PVDF Composites with Electric In Situ Poling for Pressure Sensor Applications, *Macromol. Mater. Eng.* **302** (11), 1700229 (2017).

[15] S. K. Mandal, S. Singh, R. Debnath, and P. Dey, Lead free xNiFe2O4 – (1-x) ErMnO3 (x = 0.1, 0.3 and 0.5) multiferroicnanocomposites: Studies of magnetoelectric coupling, AC electrical and magnetodielectric properties, *Ferroelect.* **536,** 77 (2018).

[16] S. K. Pradhan, A. Kumar, A. N. Sinha, P. Kour, R. Pandey, P. Kumar, and M. Kar, Study of ferroelectric properties on PVDF-PZT nanocomposite, *Ferroelect.* **516**, 18 (2017).

[17] M. B. Suresh, T. H. Yeh, C. C. Yu, and C. C. Chou, Dielectric and Ferroelectric Properties of Polyvinylidene Fluoride (PVDF)-Pb0.52Zr0.48TiO3 (PZT) Nano

Composite Films, *Ferroelect.* **381**, 80 (2009).

[18] H. S. Nalwa, Ferroelectric polymers, New York, Marcel Dekkar (1995).

[19] R. M. Briber, F. Khoury, The morphology of poly(vinylidene fluoride) crystallized from blends of poly (vinylidene fluoride) and poly(ethyl acrylate), *J. Polym. Sci: Polymer Physics* **31**, 1253 (1993).

[20] Q. Li, L. Chen, M. R. Gadinski, S. Zhang, G. Zhang, H. U. Li, E. Iagodkine, A. Haque, L. Q. Chen, T. N. Jackson, and Q. Wang, Flexible high-temperature dielectric materials from polymer nanocomposites, *Nature* **523**, 576-579 (2015).

[21] V. K. Thakur, and M. R. Kessler, Polymer Nanocomposites: New Advanced Dielectric Materials for Energy Storage Applications, in Advanced Energy Materials (John Wiley & Sons, Inc., Hoboken, NJ, USA, 2014).

[22] F. He, S. Lau, H. L. Chan, and J. T. Fan, High Dielectric Permittivity and Low Percolation Threshold in Nano-composites Based on Poly(vinylidene fluoride) and Exfoliated Graphite Nanoplates, *Adv. Mater.* **21**, 710 (2009).

[23] M. Panda, V. Srinivas, and A. K. Thakur, Role of polymer matrix in large enhancement of dielectric constant in polymer–metal composites, *Appl. Phys. Lett.* **99**, 0429051 (2011).

[24] M. Panda, V. Srinivas, and A. K. Thakur, Surface and interfacial effect of filler particle on electrical properties of polyvinylidene fluoride/nickel composites, *Appl. Phys. Lett.* **93**, 2429081 (2008).

[25] M. Panda, V. Srinivas, and A. K. Thakur, On the question of percolation threshold in polyvinylidene fluoride/ nanocrystalline nickel composites, *Appl. Phys. Lett.* **92**, 1329051(2008).

[26] M. Panda, V. Srinivas, and A. K. Thakur, Non-universal scaling behavior of polymer-metal composites across the percolation threshold, *Res. in Phys.* **05**, 136 (2015).

[27] Ch. Venketesh, V. Srinivas, M. Panda, and V. V. Rao, *Sol. Stat. Comm.* **150**, 893 (2010).

[28] M. Panda, V. Srinivas, and A. K. Thakur "Universal microstructure and Conductivity relaxation of Polymer-Conductor composites across the percolation threshold" *Current Applied Physics*, **14**, 1596 (2014).

[29] M. Panda, Evidence of a third kind of Johnscher's like universal dielectric response, *J. Adv. Dielect.* **8**, 1850028 (2018).

[30] M. Panda, and S. Soni, A Comparative Study of Visco-Elastic Properties of non-Polar and Polar Polymer Dielectrics" *Materials Today: Proceeding* **05**, 2123 (2018).

[31] Z.-M. Dang, H.-Y. Wang, and H.-P. Xu, Influence of silane coupling agent on morphology and dielectricproperty in BaTiO3/polyvinylidene fluoride composites, *Appl. Phys. Lett.* **89**, 112902 (2006).

[32] M. Panda, A. Mishra, and P. Shukla, Effective enhancement of dielectric properties in cold-pressed polyvinyledene fluoride/barium titanate nanocomposites, *SN Applied Sciences* **1**, 230 (2019).

[33] M. Panda, Major role of process conditions in tuning the percolation behavior of polyvinylidene fluoride-based polymer/metal composites, *Appl. Phys. Lett.* **111**, 0829011 (2017).

[34] Y. Bai, Z. Y. Cheng, V. Bharati, H. S. Xu, and Q. M. Zhang, High-dielectric-constant ceramic-powder polymer composites, *Appl. Phys. Lett.* **76**, 3804 (2000).

[35] C. K. Chiang and R. Popielarz, Polymer Composites with High Dielectric Constant, *Ferroelect.* **275**, 1 (2002).

[36] L. Zhang, D. Xiao, and J. Ma, Dielectric Properties of PVDF/Ag/ BaTiO3 Composites; *Ferroelect.* **455,** 77 (2013).